IOP Conf. Series: Journal of Physics: Conf. Series **1224** (2019) 012047 doi:10.1088/1742-6596/1224/1/012047

Preliminary DNS results of friction factor at low Re inside a rectangular channel with 1:10 Aspect Ratio

F. Vignati, P. Gramazio, L. Vitali, D. Fustinoni, A. Niro
Dipartimento di Energia, Politecnico di Milano, Milan, Italy
E-mail: federica.vignati@polimi.it

Abstract. A numerical and experimental study is carried on to investigate the fluid-dynamical performanced of a smooth duct with Aspect Ratio of 10. The flow Reynolds number is between 470 and 14500, computed over the duct hydraulic diameter, ranging from laminar to turbulent flow. Direct Numerical Simulations are performed, to explore the details of all flow scales, by means of a code developed at Politecnico di Milano.

The presented numerical results include the computation of the friction factor and the identification of the transition from laminar to turbulent flow regime, and reproduce experimental and literature data fairly well. The setup of the described numerical and experimental techniques will allow to carry on a detailed investigation of the fluid-dynamical and thermal performances of ribbed duct.

1. Introduction

The investigation of the enhancement of heat transfer by means of natural convection cannot leave turbulence out of consideration [1]. Due to the complex nature of the latter, the numerical study may offer a deeper knowledge of the fluid-dynamics details [2–6]. For this reason, Direct Numerical Simulations (DNS) are performed to study the flow in a rectangular duct with smooth walls and an Aspect Ratio (AR) of $1:10$, at Reynolds number up to 20000, which has not been deeply investigated yet. The goal of this article is a first assessment on the flow features, with a particular focus on the friction factor.

This work is included in a long-term campaign carried out at the ThermALab of Energy Department of Politecnico di Milano on the enhancement of heat transfer in forced convection of air flows through rectangular ducts by means of square ribs in large variety of geometrical configurations. It represents the first numerical investigation, and it can rely on a wide experimental database obtained within the described campaign, where the Nusselt number and the friction factor were measured. The ribs are adopted to enhance heat transfer by promoting to turbulence, and this results in a larger value of Nusselt, but also of the friction factor. For each flow Reynolds number, a large

number of rib geometries and configurations were tested, since the program was aimed at investigating the optimal rib configuration, i.e., producing the best compromise between the heat transfer enhancement and the induced pressure drop. Comparison with experimental data obtained in a duct with the same geometry and operating conditions are also presented. For this reason, Direct Numerical Simulations should be performed, to gain a further insight in the physics of the phenomenon. This work, therefore, represents the first step in the setup of a set of the numerical tools, whose final goal is the investigation of the ribs effects on the flow Nusselt number.

2. Overview on the investigated problem

2.1. Description of the problem

Pressure drop is obtained by studying the characteristics of forced flow in a duct characterized by an Aspect Ratio AR $= {}^{L_y}/_{2\delta}$ of 10 and a total length L_x of 2400 mm, 1000 of which dedicated to the pressure measurement. The duct cross-section is $L_y = 120.0$ mm-wide in the $y-$direction and $2\delta = 12.0$ mm-high in the $z-$direction, consisting of a hydraulic diameter D_h of 21.82 mm.

The pressure drop refers only to fully developed-flow regime, either laminar or turbulent. The Reynolds number $\mathrm{Re_D}$ is computed over the hydraulic diameter D_h, the bulk velocity U_b –computed from the mass flow rate $\dot{m}$– and the kinematic viscosity ν, and it ranges from 470 to 14500. The combination between the selected Aspect Ratio and the range of $\mathrm{Re_D}$ allows to observe the transition from laminar to turbulent flow in a duct characterized by an Aspect Ratio that has been considered, for a long time, sufficiently large to produce a quasi-two-dimensional flow, but which was recently proved to suffer from three-dimensional effects [7–10]. To study the described problem, two approaches were adopted: numerical simulations, described in section 2.2, and experimental investigation, outlined in section 2.3.

2.2. Numerical simulations

The duct flow was simulated by means of a Finite Difference solver for three-dimensional, unsteady, incompressible [11] Navier-Stokes equations, which adopts a DNS approach, developed at the Department of Aerospace Science and Technology of Politecnico di Milano [12, 13] for the simulation of channel flows. The code was then adapted by the authors to simulate duct flows, too.

In the spanwise direction, zero velocity is imposed on both walls, to comply non-penetration and no-slip boundary conditions, and the derivative of the pressure in the normal direction is set to zero [14]. In the streamwise direction, periodic boundary conditions are applied to both the velocity and the pressure field, implying a fully developed simulated flow [6, 12, 15]. While periodic velocity is commonly imposed in CFD computations of developed flows, the same consideration does not usually apply to pressure, as it would result in a pressure drop equal to zero, and hence in a meaningless null friction factor. Usually two strategies are adopted: in the first one, the pressure gradient, which is assumed uniform, is imposed, and the consequent velocity is computed, under the assumption that it is streamwise periodic. In the second approach, the pressure variation between the inlet and the outlet is set to zero, i.e., periodic boundary conditions in the streamwise direction apply to pressure, too, by introducing a body force, e.g.,

gravity acceleration, which produces a hydrostatic pressure distribution that compensate the physical pressure drop. In this second case, either the mass flow rate or the body force is unknown. The strategy adopted in this work is derived from the latter method –which allows to impose the exact value for the mass flow rate– with the additional requirement that not only $\dot{m}$ is imposed and the pressure is assumed to be streamwise periodic, but also that the driving body force is not known. To balance the introduction of the further unknown, the solution of the Navier-Stokes equation is achieved by means of a multistep procedure, which, roughly speaking, considers only one of the two unknowns per time. This allows to assume a streamwise periodic distribution of all the variables and, at the same time, to keep the mass flow rate exactly constant, as the body force depends on this constraint. A detailed description of the procedure and its validation, for the indefinite channel case, is in [16]. In the present work, an identical technique is implemented, with the difference that the second step requires the analytical solution of a Helmholtz partial differential equation over a rectangle, i.e., the duct cross section, instead of an ordinary one.

Calculations are initialized by imposing the solution for the laminar flow, $\mathbf{u} = (u, 0, 0)$, where the normalized streamwise velocity u is known [17] and results from the analytic solution of Navier-Stokes equations. A random perturbation is added during the first time steps to the laminar solution so that, if the Reynolds number is high enough, the transitions to turbulence is triggered, whereas, for low Reynolds numbers, the flow returns to a stable, laminar condition when the perturbation ceases [12, 18–21].

Numerical simulations are performed on a fixed grid, where the node spacing and the time step are selected to resolve all the flow scales [22]. To assure good accuracy of the results and stability of the calculations, a further grid refinement is performed in correspondence of the walls and the corners. The space discretization, time step setting and numerical schemeare selected in accordance with the procedures adopted in literature, e.g., [6, 12, 13, 22]. The technique adopted to force a non-oscillating mass flow rate and to compute the friction factor, briefly recalled in this paragraph, is duly described in [16].

Figure 1 shows the profiles of the streamwise component of the velocity $\overline{u}$ –made dimensionless with respect to U_b– computed at $\mathrm{Re_D} = 1018$ in the duct with $\mathrm{AR} = 10$. The displayed, dimensionless profiles are obtained by time- and streamwise-averaging 10 instantaneous fields of $\overline{u}$, with a distance of 5 time units from each others, beginning the sample after the switching-off of the perturbation, and they overlap fairly well with the instantaneous, analytic field, as depicted in figure 1.

2.3. Experimental features

The duct, whose geometrical parameters are described in section 2.1, is made of four Plexiglas plates, with a 10 mm thickness to ensure the rigidity of the structure despite the relevant duct length. Figure 2 sketches the configuration of the test rig (not to scale).

The friction factor is estimated by measuring the pressure drop along the 1000 mm-long central section of the duct. Room air enters the test section after a 1000 mm-long section aimed at allowing the full development of the boundary layers. No discontinuity is allowed between the development and the test section, to avoid the introduction of

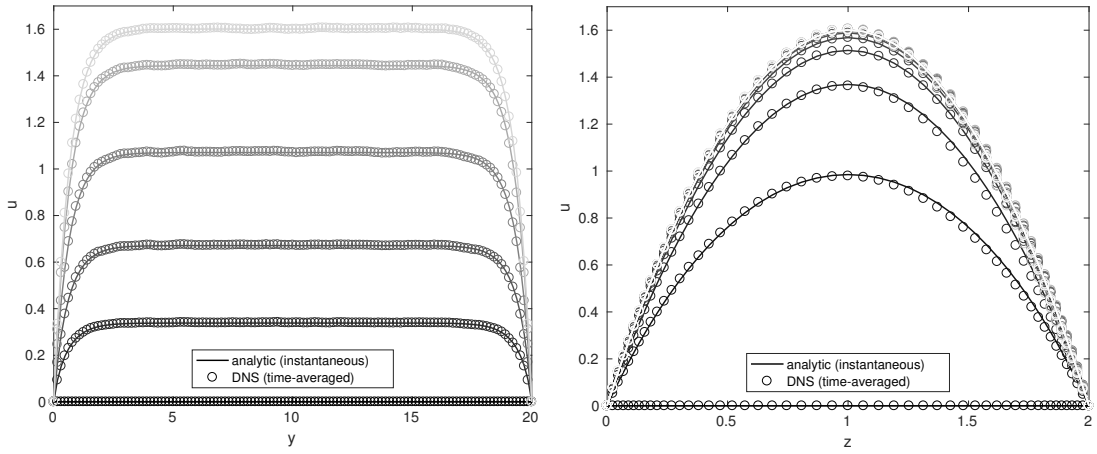

(a) (b)

Figure 1. Comparison between numerical (∘) and analytic (full line) profiles of time-averaged, dimensionless $\overline{u}$ in laminar flow regime, at $\mathrm{Re_D} = 1018$. The streamwise velocity is represented (a) versus y and (b) versus z, i.e., the spanwise and height directions respectively, made dimensionless with δ. The velocity is downsampled, to better highlight the node-value of DNS results, and it is represented along (a) 10 $z-$normal and (b) 30 $y-$normal, equally spaced planes.

false perturbation. At the centerline of both the entry and the exit section of the test section, two stations for the measurement of the pressure are located, each consisting in two pressure taps, i.e. 1 mm-diameter holes, respectively on the top and on the bottom walls of the duct.

At the coupling between the entry section and the test section, and between the latter and the exit section, two stations for the measurement of the pressure are located, each consisting in a single-leg U-tube micromanometer. The micromanometer is specifically designed and produced at the ThermALab of Energy Department of Politecnico di Milano.

To achieve the reading, an electric motor is located on the top of the smaller cylinder, which moves a needle along the reservoir axis by means of a worm gear. An electric tension is imposed between the needle and the water free surface, so that the contact between them triggers the reading of the needle position.

The micrometer sensitivity is about $1\,\mu\mathrm{m_{H2O}}$, which corresponds to a pressure variation of 0.01 Pa. The overall accuracy of the test rig is of the order of $10\,\mu\mathrm{m_{H2O}}$, as computed after a statistical analysis, considering both technical features (the resolution of the electric engine and the geometrical features of the worm gear) and side effects of the measurement setup, e.g., water evaporation, mechanical vibrations and tolerances, shape of the needle, leakages and air compressibility. It is worth noticing that the order of magnitude of the accuracy is comparable with the effect of the hydrostatic pressure difference between the top and the bottom of the duct.

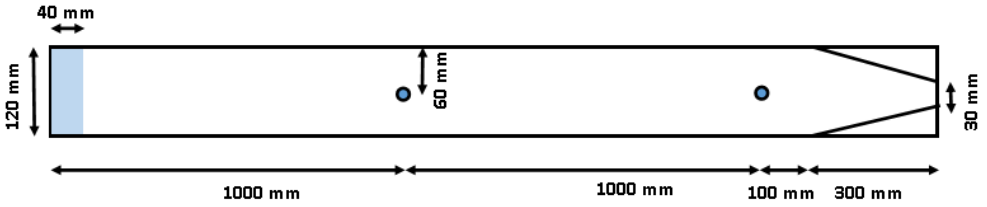

(a)

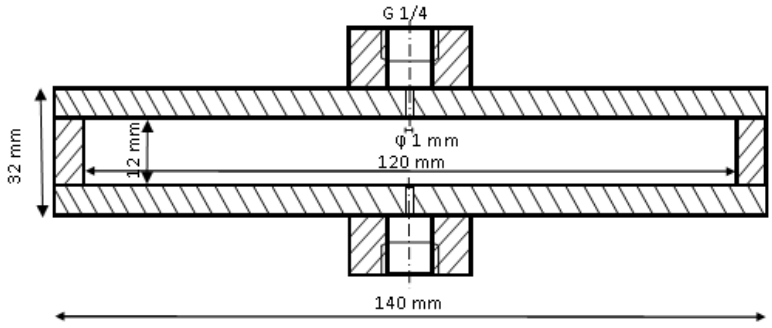

(b)

Figure 2. Sketches of the test rig for the measurement of the friction factor of a rectangular duct with AR = 10: (a) top and (b) front view (not to scale). In fig. 2(a) the flow is from left to right, and the gray dots represents the position of the pressure taps. The connection between the micromanometer taps and the duct is provided by means of threads, depicted in fig. (b).

3. Results

In the experimental framework, the estimation of Fanning friction factor f_F is performed by means of four pressure measurements: at the inlet section, the pressure is measured in correspondence of the centerplane in the spanwise direction, respectively on the top and on the bottom wall. The mean between the two results is assumed to represent the flow pressure in the considered section. The same procedure is performed at the outlet section. The friction factor is then computed by taking the slope of the straight line which interpolates between these two pressure values, and by making this result dimensionless. Unfortunately, the same procedure cannot be followed in numerical simulations, where the periodic boundary conditions impose that the pressure at every node of the outlet section is equal to the pressure evaluated at the corresponding position on the inlet surface. To estimate the friction factor, therefore, the forces across the duct are balanced, so that the force induced by the pressure drop is equivalent to the integration of non-normal stresses along lateral walls. The latter are computed as a function of the mean normal derivatives of $\overline{u}$ with respect to the walls, i.e. $\widetilde{u_z}$ and $\widetilde{u_y}$, resulting in the final expression of f_F:

$$f_F = \frac{f_D}{4} = \frac{1}{2 \cdot \mathrm{Re_D}} \left(\widetilde{u_z} + \frac{\widetilde{u_y}}{\mathrm{AR}} \right) \cdot \left(\frac{4 \cdot \mathrm{AR}}{\mathrm{AR} + 1} \right)^2$$

In figure 3(a), the friction factor is displayed versus $\mathrm{Re_D}$ for the rectangular duct in laminar flow. Calculations were performed on a single core of a sixteen-core Xeon E5 2.4 GHz CPU, with 1.5 GB RAM. The time required by the $\mathrm{Re_D} = 3636$-case is of about 10 days. For the same case, the grid resolution is 150 x 500 x 150, in x, y and z, respectively. DNS results are compared with theoretical [23] and experimental results, obtained at the ThermALab of Energy Department of Politecnico di Milano, resulting in good agreement. Figure 3(b) focuses on f_F in terms of the numerator of the analytic expression of the friction factor in laminar conditions, that is $f = {}^{C}/_{\mathrm{Re_D}}$, where the numerator C depends on the duct Aspect Ratio only. The value of C is computed from DNS results, over three $\mathrm{Re_D}$, i.e., $472, 1018$ and 2036, for Aspect Ratios of $1, 2, 5, 10, 20, 50$ and for the indefinite channel. Since the latter is known to exhibit homogeneous features in the spanwise direction, numerical simulations of the indefinite channel are carried out with different parameters: in the spanwise direction, the no-slip condition which indicates the presence of walls is substituted by periodic conditions, which allow both slip and penetration at the boundaries. This allows to assume the channel to extend indefinitely, instead of up to $\mathrm{AR}\cdot\delta$. According to [6], the computational domain size for the simulation of the indefinite channel is $4\pi\delta$ x δ x $2\pi\delta$, in x, y and z, respectively. DNS data agree fairly well with analytic values of C (the maximum error

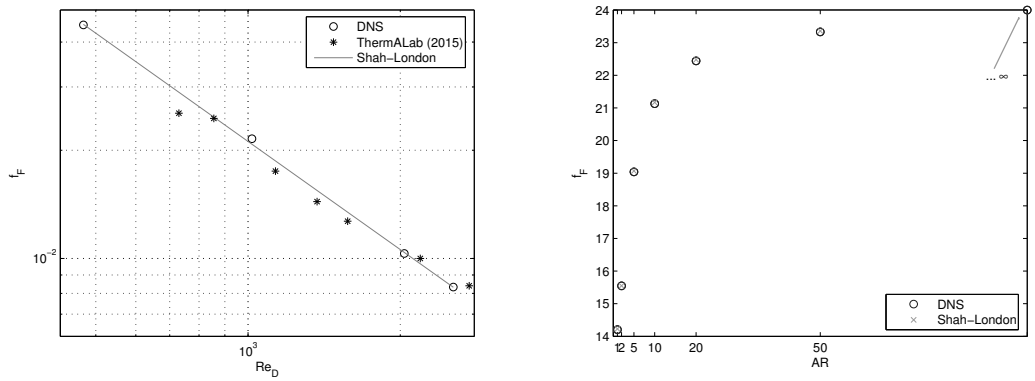

(a) (b)

Figure 3. Comparison between numerical ($\circ$), theoretical and experimental valued of Fanning friction factor for laminar flow in rectangular ducts. (a) f_F versus $\mathrm{Re_D}$ for $\mathrm{AR} = 10$; (b) C versus AR and parametrized over $\mathrm{Re_D}$. The dependence of C on $\mathrm{Re_D}$, which is theoretically null, is low enough in DNS results to be not visible in fig. (b).

between theoretical and numerical values of C is 0.2 %, for $\mathrm{AR} = 2$ and $\mathrm{Re_D} = 2036$), and the variance due to $\mathrm{Re_D}$ is totally negligible.

A further method for the estimation of f_F depends on the adopted numerical technique, and consists in determining the correction to the pressure term, at each time step, required to satisfy the prescribed, constant mass flow rate. The computation of the pressure correction is detailed and duly discussed in [16].

Figure 4 compares the friction factors, as resulting from DNS simulations for diverse values of $\mathrm{Re_D}$, obtained by means of the two described methods. As expected, the

numerical values are in good agreement, and indicate the values of $\mathrm{Re_D}$ between 2500 and 4500 as the range where the laminar-turbulent flow transition occurs.

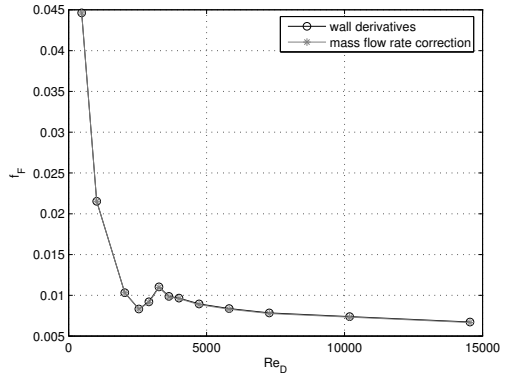

Figure 4. Fanning friction factor of a duct flow with AR = 10 at $\mathrm{Re_D}$ between 470 and 14500, obtained by means of DNS study. The two methods are compared: the wall derivatives of $\overline{u}$ ($\circ$) and the mass flow rate correction ($*$).

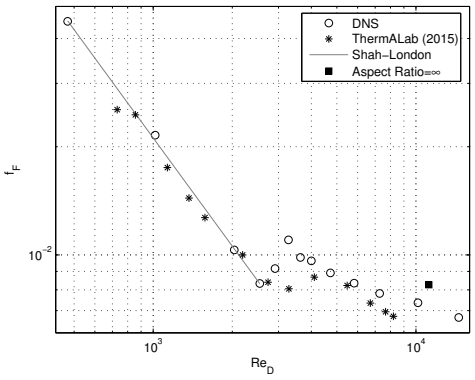

Figure 5. Comparison between DNS results and experimental data obtained at ThermaLab of Politecnico di Milano for the Fanning friction factor of a duct flow with AR = 10 at $\mathrm{Re_D}$ between 470 and 14500.

Eventually, numerical data are assessed against experimental valued for f_F obtained at ThermALab of Energy Department of Politecnico di Milano, as depicted in figure 5. The accordance between numerical and experimental data is not exact, since a deviation occurs at high Reynolds numbers. This discrepancy is probably due to the procedure adopted to estimate the experimental value of f_F, which is based on pressure measurements only along the centerline, and which therefore neglects the non-uniform distribution of the flow in the spanwise direction [7–10, 24–26]. Table 1 reports the deviations of numerical and experimental data with respect to the analytic solution (only in laminar flow) or between DNS and experimental results, computed on Fanning friction factor. The relative difference margin, even in the worst case, is below 9 %, which is in the commonly accepted range, considering also the differences between the numerical and the experimental procedures.

4. Conclusions

Direct Numerical Simulations are carried out to investigate the flow feature in a rectangular duct with Aspect Ratio of 10. The Reynolds number covers laminar flow, the transition to turbulence and "slow" turbulent flows, ranging from 470 to 14500. This work is motivated by the low number of literature on flows in correspondence of the laminar-turbulent transition in ducts with AR = 10, which is borderline to consider the internal flow to show approximately two- or fully three-dimensional features. The novel numerical code consists in a Finite-Difference solver for unsteay, incompressible, Navier-Stokes equations on structured grids, based on the code previously developed at

Table 1. Relative differences between the computed values of Fanning friction factor. The first comparison concerns the average error between analytical values, which are known in laminar conditions, and numerical (for err_{an-DNS}) or experimental (for $\mathrm{err}_{an-exper}$) data. The average relative differences between numerical and experimental data, either in laminar or in turbulent conditions, are quantified by $\mathrm{err}_{DNS-exper,L}$ and $\mathrm{err}_{DNS-exper,T}$, respectively.

err_{an-DNS}	1.1849 %
$\mathrm{err}_{an-exper}$	5.9441 %
$\mathrm{err}_{DNS-exper,L}$	8.2906 %
$\mathrm{err}_{DNS-exper,T}$	8.6916 %

Politecnico di Milano for the direct turbulence simulation of channel flows, and adapted for the simulation of duct flows.

The Fanning friction factor is computed at diverse values of $\mathrm{Re_D}$. The agreement between DNS and experimental results is good but not perfect, probably due to the different approaches adopted to compute f_F.

The provided solutions can be further improved, not only by refining the investigation tools (e.g., by adopting Compact Finite Differences or even longer computational domains, for the DNS), but in particular by unifying as much as possible the experimental and the numerical investigations. Since this work belongs to a long-time research campaign carried on at the ThermaLab of Politecnico di Milano, the final goal is to introduce in the code the simulation of more complex, non isothermal duct flows.

References

[1] Webb R L 1994 *Principles of enhanced heat transfer* (New York: Winley-Interscience)
[2] Rodi W, Mansour N N 1993 Low Reynolds number $k-\varepsilon$ modelling with the aid of direct simulation data *J. Fluid Mech.* **250** 509
[3] Mansour N N, Kim J, and Moin P 1988 Reynolds-stress and dissipation rate budgets in a turbulent channel flow *J. Fluid Mech.* **194 15-44**
[4] Blackburn H M, Mansour N N and Cantwell B J 1996 Topology of fine scale motions in turbulent channel flow *J. Fluid Mech.* **310** 269
[5] Kim J and Antonia R A 1993 Isotropy of the small scales of turbulence at low Reynolds number *J. Fluid Mech.* **251** 219
[6] Kim J, Moin P and Moser R D 1987 Turbulence statistics in fully developed channel flow at low Reynolds number *J. Fluid Mech.* **177** 133
[7] Vinuesa R, Noorani A, Lozano-Durn A, El Khoury G K, Schlatter P, Fischer P F and Nagib H M 2014 Aspect ratio effects in turbulent duct flows studied through direct numerical simulation *J. of Turbulence* **15.10** 677-706, doi:10.1080/14685248.2014.925623
[8] Vinuesa R 2013 Synergetic computational and experimental studies of wall-bounded turbulent flows and their two-dimensionality *PhD thesis, Illinois Institute of Technology*
[9] Vinuesa R, Bartrons E, Chiu D, Dressler K M, Redi J D, Suzuki Y, Nagib H M 2014 New insight into flow development and two dimensionality of turbulent channel flows *Exp. Fluids* **55** 1759 https://doi.org/10.1007/s00348-014-1759-8
[10] Vinuesa R, Schlatter P and Nagib H M 2015 Characterization of the secondary flow in turbulent

rectangular ducts with varying aspect ratio *Int. Symposium on Turbulence and Shear Flow Phenomena (TSFP-9), June 30-July 3 2015, Melbourne, Australia*

[11] Shirokoff D and Rosales R R 230 An efficient method for the incompressible Navier-Stokes equations on irregular domains with no-slip boundary conditions, high order up to the boundary *J. Comput. Phys.* **230** 8619-46

[12] Luchini P and Quadrio M 2006 A low-cost parallel implementation of direct numerical simulation of wall turbulence *J. Comput. Phys.* **211.2** 551-71

[13] Monti C M 2017 Metodo dei contorni immersi per la simulazione numerica diretta di correnti turbolente su pareti non piane *MSc thesis, Politecnico di Milano*

[14] Anders Petersson N 2001 Stability of Pressure boundary Conditions for Stokes and NavierStokes Equations *J. Comput. Phys.* **172** 40-70

[15] Quadrio M and Luchini P 2001 A $4-th$ order accurate, parallel numerical method for the direct simulation of turbulence in cartesian and cylindrical geometries *Proc. of the XV AIMETA Conf. on Theor. Appl. Mech*

[16] Quadrio M, Frohnapfel B, Hasegawa Y 2016 Does the choice of the forcing term affect flow statistics in DNS of turbulent channel flow? *European J. of Mech. B/Fluids* **55** 286-293

[17] Shah R K and London A L 1978 *Laminar Flow Forced Convection in Ducts - A Source Book for Compact Heat Exchanger Analytical Data* (New York: Academic Press, Inc)

[18] Orszag S A 1971 Accurate solution of the OrrSommerfeld stability equation *J. Fluid Mech.* **50.04** 689-703

[19] Uhlmann M and Nagata M 2006 Linear stability of flow in an internally heated rectangular duct *J. Fluid Mech.* **551** 387-404 doi:10.1017/S0022112005008487

[20] Theofilis V, Duck P W and Owen J 2004 Viscous linear stability analysis of rectangular duct and cavity flows *J. Fluid Mech.* **505** 249-286 doi:10.1017/S002211200400850X

[21] Tatsumi T and Yoshimura T 1990 Stability of the laminar flow in a rectangular duct Journal of Fluid Mechanics *J. Fluid Mech.* **212** 437-449 doi:10.1017/S002211209000204X

[22] Comini G, Croce G and Nobile E 2008 *Fondamenti di termofluidodinamica computazionale* (S.G.E)

[23] Muzychka Y S, Yovanovich M M 2009 Pressure drop in laminar developing flow in noncircular ducts: a scaling and modeling approach *J. Fluid Eng.* **131** 111105.1-9

[24] Dean R B 1978 Reynolds number dependence of skin frictin and other bulk flow variables in two-dimensional rectangular duct flow *J. Fluid Eng.* **100** 215

[25] Bradshaw P and Hellens G E 1964 The N.P.L. 59 in x 9 in boundary layer tunnel *N.P.L. Aero Report* **1119**

[26] Monty J P 2005 Developments In Smooth Wall Turbulent Duct Flows *PhD thesis, University of Melbourne*